Received: 13 June 2022 | Revised: 2 January 2023 | Accepted: 14 January 2023

DOI: 10.1002/joc.8020

RESEARCH ARTICLE

International Journal of Climatology RMetS

Extreme precipitation records in Antarctica

Sergi González-Herrero[1,2,3] | **Francisco Vasallo**[2] | **Joan Bech**[1,4] | **Irina Gorodetskaya**[5,6] | **Benito Elvira**[2] | **Ana Justel**[7]

[1]Department of Applied Physics—Meteorology, University of Barcelona, Barcelona, Spain

[2]Antarctic Group, Spanish Meteorological Agency (AEMET), Spain

[3]WSL Institute for Snow and Avalanche Research SLF, Davos, Switzerland

[4]Water Research Institute, University of Barcelona, Barcelona, Spain

[5]Centre for Environmental and Marine Studies (CESAM), Department of Physics, University of Aveiro, Aveiro, Portugal

[6]Interdisciplinary Centre of Marine and Environmental Research (CIIMAR), University of Porto, Matosinhos, Portugal

[7]Department of Mathematics, Universidad Autónoma de Madrid, Madrid, Spain

Correspondence
Sergi González-Herrero, WSL Institute for Snow and Avalanche Research SLF. Flüelastrasse 11, 7260 Davos Dorf, Switzerland.
Email: sergi.gonzalez@slf.ch

Funding information
Agencia Estatal de Investigación; European Regional Development Fund, Grant/Award Numbers: CGL2015-65627-C3-1-R, CGL2015-65627-C3-2-R, RTI2018-098693-B-C32, PID2020-116520RB-I00; Generalitat de Catalunya; Ministério da Ciência, Tecnologia e Inovação; Fundação para a Ciência e a Tecnologia, Grant/Award Numbers: CIRCNA/CAC/0273/2019, UIDP/04423/2020, UIDB/04423/2020, LA/P/0094/2020, UIDB/50017/2020, UIDP/50017/2020

Abstract

Monitoring extreme precipitation records (EPRs), that is, the most extreme precipitation events, is a challenge in Antarctica due to the reduced number of stations available in the continent and the limitations of the instrumentation for measuring solid precipitation. Still, extreme precipitation events may contribute substantially to the variability of ice sheet snow accumulation and even may cause important ecological impacts. This article presents the Antarctic EPRs at different temporal scales, studying the relationship between precipitation amount and temporal duration through a power scaling law, ranging from 1 day to 2 years. This is achieved using precipitation datasets from the ERA5 reanalysis and the RACMO2 regional climate model. Moreover, we present a selection of EPRs case studies examining the synoptic mechanisms that produce such events in Antarctica. Despite ERA5 EPRs are usually lower than those found in RACMO2, they present similar scaling exponents. EPRs are found in Loubet and south Graham Coasts, in the central section of the Antarctic Peninsula, and in the north of Alexander Island, where orographic enhancement increases precipitation amounts. As expected, Antarctic EPRs are much lower than world-wide EPRs, ranging from 6 to 10% at short temporal scales (from 1 to 10 days) and from 10 to 20% at long temporal scales (from 90 days to 2 years) in ERA5. Regional variability of extreme precipitation scaling exponents show similar spatial patterns than previously calculated precipitation concentration. On the other hand, the lack of summer events in Antarctic EPRs evidences that stronger fluxes in winter play a key role on extreme precipitation during EPR events, which are mainly produced by long-range transport of moisture by atmospheric rivers impinging on Antarctic mountains.

KEYWORDS

Antarctica, atmospheric rivers, extreme precipitation, scaling law, weather records

1 | INTRODUCTION

Monitoring extreme weather records is of paramount importance to assess Earth's climate change and, particularly, to determine possible trends in extreme events (Cerveny *et al.*, 2007), which have the potential for impacting ecological systems (McPhillips *et al.*, 2018). For this reason, the World Meteorological Organization (WMO) Commission for Climatology created a database to archive and verify the world weather record extremes (WMO, 2022). To date, the only continental value in this database that has not been determined yet is the highest average yearly precipitation in Antarctica, which is estimated to exceed 800 mm according to a modelling study performed by Bromwich *et al.* (2004). The unavailability of this measure is due to the unique combination of difficulties that lead to large uncertainties in precipitation estimates in Antarctica. On one side, limited accessibility and the harsh climate affect the unmanned instrumentation and limit the automatic measurement of precipitation (Tang *et al.*, 2018a). On the other side, the deflection of snow particles over the gauge at high wind speed produce a large undercatch of the precipitation making it difficult to measure using traditional methods (Folland, 1988; Kochendorfer *et al.*, 2017). The lack of in situ measurements produces a great discrepancy in the precipitation amounts in the different reanalyses on the continent (Behrangi *et al.*, 2016).

Temporal scaling of extreme precipitation records (EPRs) is also by itself a relevant research topic since Jennings (1950) presented the world extreme rainfall records for different durations between 1 min and 2 years. The study showed a linear relationship between the maximum precipitation amount P and the temporal duration D in a log–log space so that data followed a power law equation:

$$P = a D^b, \tag{1}$$

where b is the scaling coefficient. Paulhus (1965) confirmed this relationship and fitted an updated list of records to an envelope curve with a scaling exponent of 0.475. A formal mathematical approach to estimate the envelope was proposed by Gonzalez and Bech (2017). This power law function, often referred to Jennings' power law, has been the object of analysis by studies using point gauge measurements (Hubert *et al.*, 1993; Galmarini *et al.*, 2004; Zhang *et al.*, 2013b), satellite precipitation estimates (Breña-Naranjo *et al.*, 2014), weather radar data (Pöschmann *et al.*, 2021) or climate models (Zhang *et al.*, 2013a). Regional and seasonal variability of extreme precipitation in mid-latitude countries has also been studied using extended databases (Gonzalez and Bech, 2017) or single stations (Casas *et al.*, 2010; Pérez-Zanón *et al.*, 2016). The scaling of precipitation has been explained in a framework of physical complex systems as a self-organized critical process, such as other natural processes like earthquake magnitude, landslides and hurricane dissipation (Hubert *et al.*, 1993; Peters *et al.*, 2002; Peters and Christensen, 2002; Corral *et al.*, 2010).

Evaluating records in Antarctica is important because they determine the limits of the atmospheric system of the continent. Precipitation is a major positive component of the surface mass balance (SMB) of the ice sheet and glaciers (Lenaerts *et al.*, 2012; Frieler *et al.*, 2015; Gorodetskaya *et al.*, 2015) and climate model projections predict an increase of the Antarctic precipitation over the continent by the end of the 21st century (Krinner *et al.*, 2007; Uotila *et al.*, 2007; Ligtenberg *et al.*, 2013; Lenaerts *et al.*, 2016). This increase is expected to be dominated by synoptic scale events, which will carry more moisture from lower latitudes with increasing air temperature following the Clausius–Clapeyron relation (Dalaiden *et al.*, 2020). The most extreme synoptic scale events contribute significantly to the total annual precipitation (Turner *et al.*, 2019) accounting for 70% of the explained variance of the annual precipitation in the whole continent (Turner *et al.*, 2019). The majority of extreme precipitation events at the coast is associated with atmospheric rivers, which consist of anomalous moisture flux organized in narrow and long corridors typically in the pre-cold front zone of the extra-tropical cyclones' warm sector (Gorodetskaya *et al.*, 2014; Wille *et al.*, 2021). The frequency and intensity of the atmospheric rivers is projected to increase in the future (Espinoza *et al.*, 2018; O'brien *et al.*, 2022), and thus it is important to explore their association with extreme precipitation. Extreme precipitation events in Antarctica have been analysed on an event basis (Schlosser *et al.*, 2010; Yu *et al.*, 2018), while the most extreme precipitation records for different temporal durations in this continent have not been analysed yet.

As the observational datasets of surface precipitation in Antarctica are very limited, in this article, we study the most extreme precipitation records at different temporal scales from 1 day to 2 years based on reanalysis and numerical modelling datasets. We estimate the scaling law relationship that associates Antarctic precipitation extremes to different temporal periods and analyse the spatial distribution of the scaling exponent in the Antarctic continent comparing our results with the extreme precipitation events calculated by Turner *et al.* (2019). Finally, we briefly analyse a selection of case studies covering the most extreme precipitation events occurred in the continent.

2 | DATA AND METHODS

2.1 | Datasets

This subsection presents the two datasets used for the analysis—ECMWF Reanalysis 5th generation (ERA5; Hersbach *et al*., 2020) and Regional Atmospheric Climate Model v2.3 (RACMO2; van Wessem *et al*., 2014)—in the Antarctic domain (poleward of 60°S) for the period from January 1979 to July 2017.

ERA5 is the fifth generation of meteorological reanalysis of the European Centre for Medium-Range Weather Forecasts (ECMWF), has a horizontal resolution of 0.25° (about 30 km), and is based on the Integrated Forecasting System (IFS) Cy41r2. The large-scale precipitation parametrization used is an improved version of the Tiedtke (1993) scheme, with independent liquid and ice water contents and a single-moment microphysics scheme. A recent evaluation of the large-scale performance with respect to the CloudSat satellite-borne radar-derived precipitation measurements indicates that ERA5 presents a positive bias in annual precipitation, especially over the plateau but it captures well the observed seasonality (Roussel *et al*., 2020). Another evaluation over the Southern Ocean indicates that ERA5 shows more snowfall and less rainfall than other reanalysis, but the precipitation patterns are, in general, well captured (Boisvert *et al*., 2020).

The same analysis has also been performed using the RACMO2 regional climate model precipitation outputs for the same period. The RACMO2 version used in this study combines the dynamical core of the HIRLAM model version 6.3.7 with the ECMWF IFS physics cycle Cy33r1 forced by the ERA-Interim reanalysis data as boundary conditions (Van Wessem *et al*., 2014). RACMO2 has a horizontal resolution of 27 km, comparable to the ERA5. With other regional climate models driven by ERA-Interim, it increases the precipitation of the forcing model (Mottram *et al*., 2021). Evaluations of the SMB (precipitation minus evaporation and sublimation) show that RACMO2 represents well the snow accumulation over the Antarctic Plateau but presents an overestimation at some coastal regions (Wang *et al*., 2016).

To interpret the results, we included the global EPRs (the greatest observed point) precipitation values for the world from the Hydrometeorological Design Studies Center of the National Oceanic and Atmospheric Administration (NOAA-HDSC) (NWSa, 2022a). We also included comparisons with compilations of extreme precipitation records for different durations available for Australia (BOM, 2022), Spain (Gonzalez and Bech, 2017) and United States (NWSb, 2022b).

2.2 | Determination of EPR and scaling law

Extreme precipitation records at different temporal aggregation levels were computed using rolling sums applied over moving windows from 1 day to 2 years for each grid point of the domain considered. EPRs were obtained picking the maximum value of each temporal aggregation. The scaling law of the extreme precipitation records is expressed as in Equation (1). We estimate the coefficients of the scaling law by using the equivalent linear expression:

$$\log(P) = a + b\log(D) \tag{2}$$

and the ordinary least squares method of regression estimation (Rawlings *et al*., 1998). We also calculated the envelope line with the same slope as the fitting line, so that P was equal or greater than all observations, as described in Gonzalez and Bech (2017). This scaling law has been also evaluated for each grid point of ERA5 below 60°S, and to facilitate the comparisons we focused on 10 locations selected after Turner *et al*. (2019) using the closest grid point in ERA5 (see Table S1.1, and for further details Table 1 in Turner *et al*., 2019). Those stations were proposed as representative of different regions of Antarctica and because some of them are close to an ice core-drilling site (see their Table S1.1).

3 | PRECIPITATION RECORDS IN ANTARCTICA

Table 1 lists Antarctic EPRs from 1 day to 2 years from January 1979 to July 2017 found in ERA5 and RACMO2. Both datasets present large discrepancies in magnitude, with RACMO2 roughly doubling ERA5 EPR precipitation amount (RACMO2 to ERA5 EPR ratio ranges from 1.7 to 2.5 on all temporal scales). As there are no systematic observations of the extreme events in Antarctica to compare with, we cannot assess the performance of the EPRs found. However, RACMO2 and ERA5 sometimes agree on the EPR date for some durations, such as 3-day (15–17 July 2016) or 270-day (3 March to 27 November 2010). Despite the differences in magnitude exhibited by both datasets, they present a similar scaling exponent. To simplify the discussion, in the remainder of the manuscript we will focus only on the ERA5 dataset unless specified.

As expected, EPRs found in Antarctica in both datasets are much lower than EPRs based on the global point measurements for every duration. The proportion of the Antarctic EPRs with respect to the global EPRs in ERA5 ranges from 6% at short temporal scales to 20% at long

TABLE 1 Antarctic extreme precipitation records (EPRs) calculated from ERA5 and RACMO2, and world EPRs from NOAA-HDSC over different time scales (from 1 day to 2 years), and proportion of Antarctica to global EPRs.

Duration (days)	ERA5 Antarctic EPRs (AR)				RACMO2 Antarctic EPRs (AR)				World EPRs (WR) PCP	ERA5 AR/WR (%)	RACMO2/ ERA5 AR (%)
	PCP	LAT	LON	Date	PCP	LAT	LON	Date			
1	110.3	−66.25	−64.75	27 Mar 2017	278.8	−69.01	−70.89	16 Jul 2016	1,825	6.0	2.5
2	184.1	−66.75	−66.00	26–27 Apr 1998	381.7	−69.01	−70.89	16–17 Jul 2016	2,493	7.4	2.1
3	221.0	−69.00	−70.50	15–17 Jul 2016	488.0	−69.01	−70.89	15–17 Jul 2016	3,929	5.6	2.2
4	269.8	−69.00	−71.25	27–30 Jun 2006	533.3	−69.01	−70.89	15–18 Jul 2016	4,936	5.5	2.0
5	288.3	−69.00	−71.25	27 Jun–1 Jul 2006	613.0	−69.01	−70.89	15–19 Jul 2016	4,979	5.8	2.1
6	302.2	−69.00	−70.50	15–20 Jul 2016	655.9	−69.01	−70.89	14–19 Jul 2016	5,075	6.0	2.2
7	343.7	−66.00	−64.75	23–29 Sep 1996	690.8	−66.87	−65.88	4–10 Oct 1995	5,400	6.4	2.0
8	366.2	−66.00	−64.75	23–30 Sep 1996	744.2	−66.87	−65.88	2–9 Oct 1995	5,510	6.6	2.0
9	393.8	−66,00	−64.75	23 Sep–1 Oct 1996	846.6	−66.87	−65.88	2–10 Oct 1995	5,512	7.1	2.1
10	425.9	−66.00	−64.75	21–30 Sep 1996	904.1	−66.87	−65.88	1–10 Oct 1995	5,678	7.5	2.1
15	528.5	−66.00	−64.75	20 Sep–4 Oct 1996	1,152.0	−66.87	−65.88	26 Sep–10 Oct 1995	6,083	8.7	2.2
20	659.5	−66.00	−64.75	22 Sep–11 Oct 1995	1,416.3	−66.87	−65.88	22 Sep–11 Oct 1995	N/A	N/A	2.1
30	850.9	−66.00	−64.75	17 Oct–15 Nov 2010	1,525.1	−66.87	−65.88	20 Sep–19 Oct 1995	9,300	9.1	1.8
60	1,256.2	−66.00	−64.75	28 Sep–26 Nov 2010	2,131.2	−66.87	−65.88	1 Oct–29 Nov 1995	12,767	9.8	1.7
90	1,649.5	−66.00	−64.75	4 Aug–1 Nov 2001	2,827.7	−66.87	−65.88	7 May–4 Aug 1989	16,369	10.1	1.7
180	2,716.2	−66.00	−64.75	5 May–1 Nov 1989	4,752.6	−66.87	−65.88	30 Apr–26 Oct 1989	22,454	12.1	1.7
270	3,570.0	−66.00	−64.75	3 Mar–27 Nov 2010	6,200.2	−66.87	−65.88	3 Mar–27 Nov 2010	N/A	N/A	1.7
365	4,266.6	−66.00	−64.75	26 Feb 2001–25 Feb 2002	7,352.5	−66.87	−65.88	27 Nov 2015–25 Nov 2016	26,470	16.1	1.7
545	5,936.5	−66.00	−64.75	27 Dec 1998–24 Jun 2000	10,269.8	−66.87	−65.88	9 Feb 1998–7 Aug 1999	N/A	N/A	1.7
730	7,812.5	−66.00	−64.75	13 Mar 1998–11 Mar 2000	13,622.7	−66.87	−65.88	13 Mar 1998–11 Mar 2000	40,768	19.2	1.7

temporal scales. All global EPRs for scales over 1 day are located in the tropics (Paulhus, 1965; Quetelard *et al.*, 2009). At temporal scales from 1 to 15 days, the combination of deep moist convection, strong moisture advection and convergence into the tropical convective storms provide enough moisture to exceed rainfall amounts of 1,000 mm in 24 hr (Galmarini *et al.*, 2004; Koutsoyiannis and Papalexiou, 2017). At scales over 1 month, high air temperatures allow for greater water vapour content in the atmosphere while large-scale tropical circulations such as monsoons provide a constant input of moisture that favours heavy rainfall amounts (Galmarini *et al.*, 2004). Meteorological factors involved in precipitation processes leading to such extreme amounts do not exist in Antarctica. In contrast, precipitation is governed by large-scale moisture advection associated with extra-tropical cyclones with the strongest poleward moisture transport occurring during atmospheric blocking events which favours persistent lows (Schlosser *et al.*, 2010; Yu *et al.*, 2018; Turner *et al.*, 2019; Wille *et al.*, 2021). The majority of extreme precipitation events in Antarctica have been linked with atmospheric rivers, transient belts of anomalous poleward moisture transport sometimes linked to a series of extra-tropical cyclones typically blocked by a high pressure ridge on the east (Gorodetskaya *et al.*, 2014; Wille *et al.*, 2021). Due to low temperature, precipitation mostly occurs as snowfall with only sporadic and small amounts of rainfall or drizzle recorded in the Antarctic Peninsula and some coastal sites (Vignon *et al.*, 2021). However, anomalous warm events might trigger extensive rainfalls that can reach to the interior of the continent as in January 2016 (Nicolas *et al.*, 2017).

All EPRs identified in Antarctica using ERA5 occur in two regions of the west side of the Antarctic Peninsula characterized by steep terrain (Figure 1; Table 1; Supplementary Figure S1.1). From 1 to 6 days the EPRs are distributed in 4 precipitation events. EPR events for 1 and 2 days occurred in Loubet and south Graham Coasts, in the central section of the Antarctic Peninsula, on

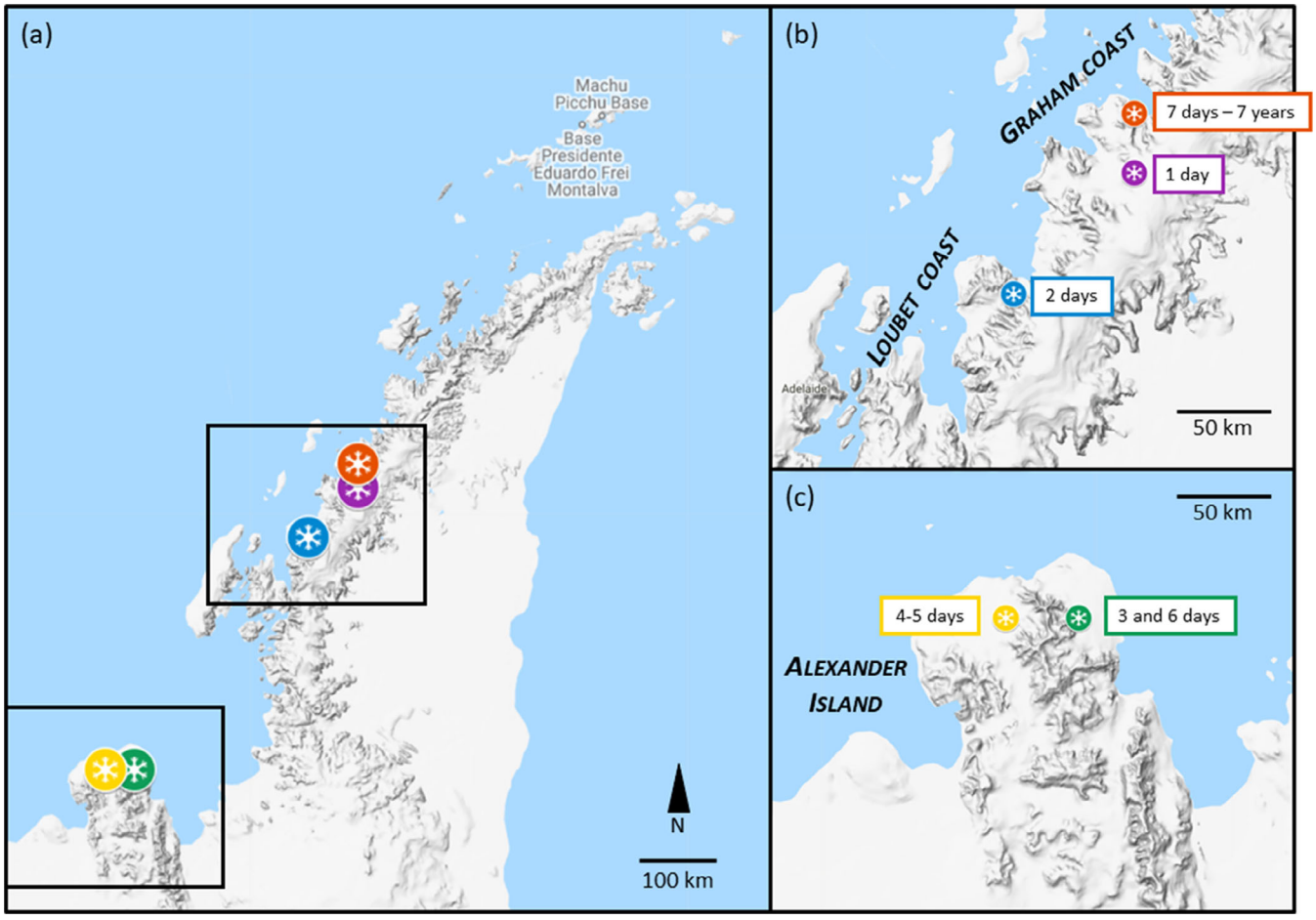

FIGURE 1 Locations of the Antarctic EPR simulated by ERA5 (see Table 1 for reference). (a) General perspective of the Antarctic Peninsula. (b) Zoom over the Loubet and Graham coasts. (c) Zoom over the north Alexandre Island. The ERA5 orography of the region appears in Supplementary Figure S1.1. Cartography from GoogleMaps. [Colour figure can be viewed at wileyonlinelibrary.com]

27 March 2017 (110 mm) and 26–27 April 1998 (184 mm), respectively. EPRs over the duration of 3–6 days occurred north of Alexander Island in two different events: 27 June to 1 July 2006 (288 mm) and 15–20 July 2016 (302 mm). The 1-day grid-point EPR in ERA5 is 110 mm, a considerable amount in a Polar region. This amount represents 6% of the global EPR. However, it is a rather low value compared with other regional point-based 1-day EPRs in mid-latitudes such as the United States (1,092 mm at Alvin, Texas) or Spain (817 mm at Oliva, Valencia) with a much longer database, especially considering the absence of deep moist convection in Antarctica. It should also be noted that the EPR found in ERA5 represents a gridbox-average (including an average topography) compared to a point measurement given by the previously mentioned EPRs.

From 7 days to 2 years, all the records are located at south Graham Coast. EPR from 7 days to 15 days are part of the same event, which ranged from September to October 1996. EPR from 20 days to 2 years correspond to different events. The 1-year EPR in ERA5 is 4,267 mm, which is 16% of the global EPR and close to other mid-latitude countries such as Spain (5,503 mm at Casas do Porto; A Coruña) and mid-latitude regions of Australia (4,998 mm at Mount Read, Tasmania). This illustrates the important role of the moisture transport events towards Antarctica coupled with the effect of the steep topography of the Antarctic Peninsula in generating the orographic enhancement of precipitation leading to EPRs.

None of the records between 1 day and 9 months occurs in summer suggesting that increased moisture capacity of the warmer air by the Clausius–Clapeyron relation does not compensate the weaker fluxes that occur in this season. Instead, the occurrence of EPRs during the cold season indicates that strong cyclone activity in the Southern Ocean with larger moisture exports from subtropical latitudes is instrumental on Antarctic EPRs (see Section 5).

4 | EXTREME PRECIPITATION SCALING AND REGIONAL VARIABILITY

Figure 2 shows the Antarctic EPR in comparison with the global EPR in a log–log plot of precipitation amount against duration (see Figure S2.1 for RACMO2). The estimated power law models are $P = 1.0\ D^{0.63}$, for Antarctic EPRs, and $P = 52.7\ D^{0.49}$, for world-wide EPRs. The envelopes are $P = 1.2\ D^{0.63}$ and $P = 73.1\ D^{049}$, respectively. In both cases, the power law relationship is statistically significant (p-values <.0001). The higher exponent for

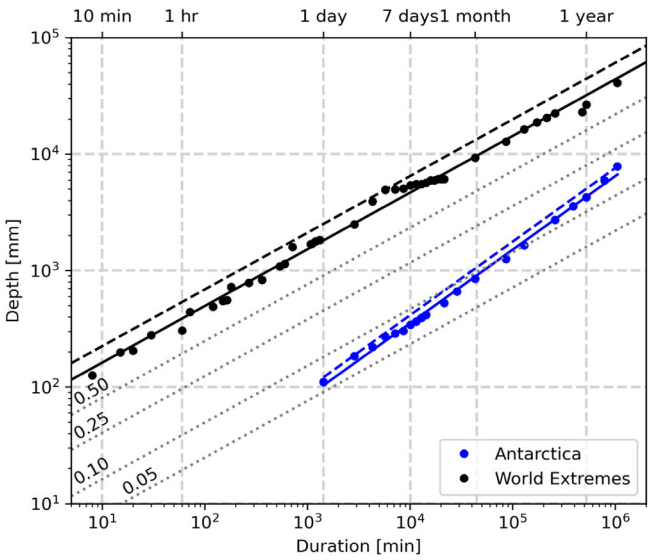

FIGURE 2 Antarctic extreme precipitation records amount (mm) versus duration (min) (blue dots), the scaling law fitting on a Log–Log plot (solid blue line) and envelope (dashed blue line). For reference, we included the World extreme precipitation records (black dots and lines) and a fraction of their fitting curve (dotted black lines). [Colour figure can be viewed at wileyonlinelibrary.com]

Antarctic EPRs suggests that extreme precipitation increases at a higher rate with duration than global EPRs and is related to a higher regularity in extreme precipitation mechanisms (Gonzalez and Bech, 2017). However, those values are only representative of a very specific region in the Antarctic Peninsula that receives much larger amounts of moisture advection compared to other regions.

To evaluate the spatial variability of the power law coefficient through the continent, we computed the local scaling at every grid point of the Antarctic region (Figure 3 and S2.2 for RACMO2). Scaling coefficients are greater than 0.60 over the Southern Ocean and generally diminish near the Antarctic coast. Values below 0.60 near the coast suggest a reduction of the regularity of extreme precipitations, probably driven by the offshore katabatic winds present on those areas (Parish and Bromwich, 2007). At the Bellingshausen Sea, the exponent ranges between 0.60 and 0.70, similar to other oceanic regions. It is noticeable the oceanic influence on the EPR at the Antarctic Peninsula illustrating the primary role of the Pacific Ocean pathway in moisture transport towards the Peninsula (Turner *et al.*, 1995). Conversely, at the Weddell Sea, the exponent drops to 0.50 suggesting a reduction of the regularity of the extreme precipitation events. This sharp change in EPR conditions is illustrated by the difference in the exponent and the magnitude between the points in the Western Antarctic Peninsula

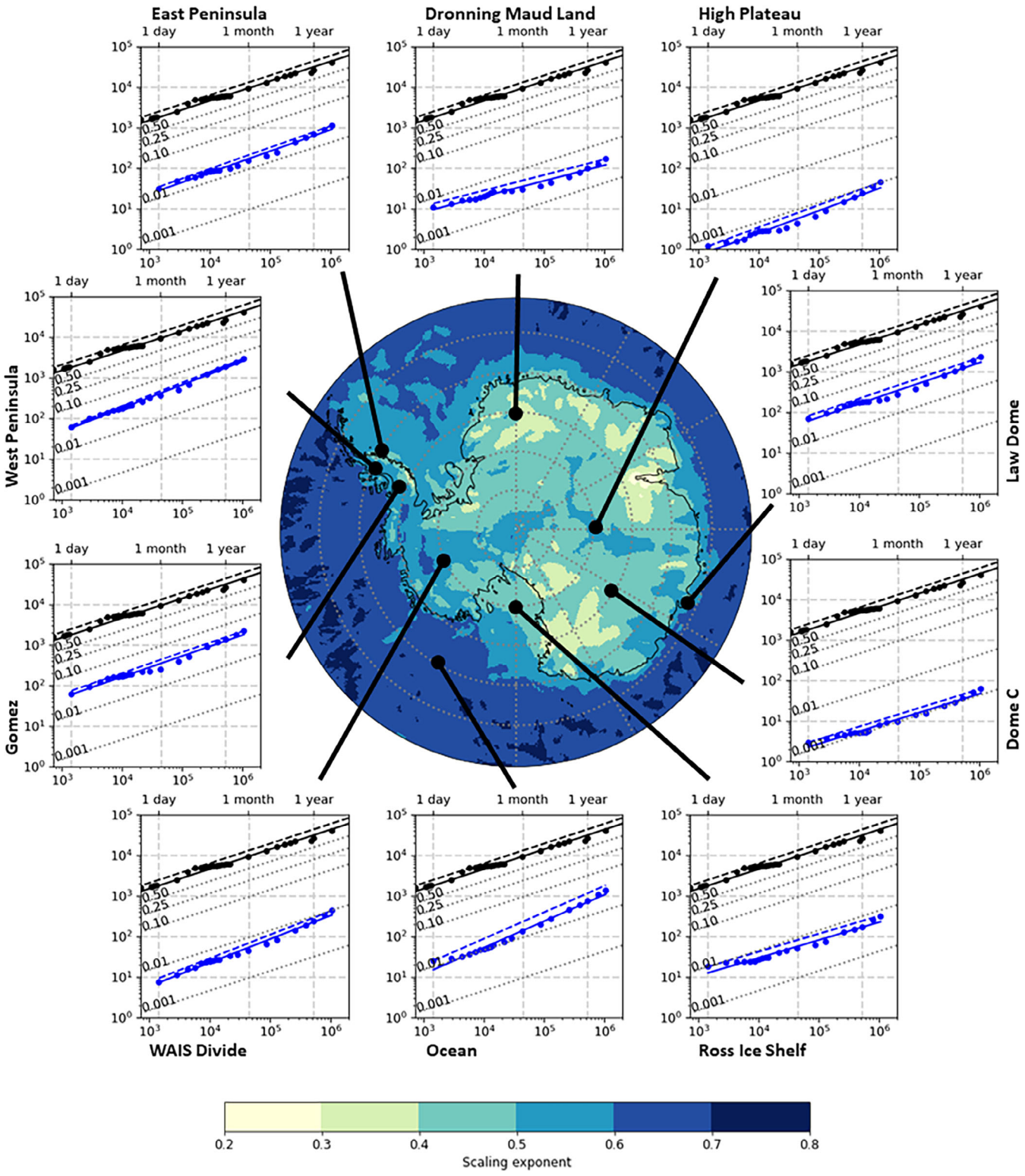

FIGURE 3 Regional variation of the power law scaling coefficient. The boxes show the local scaling law at different locations. Location information can be found in Table 1 at Turner *et al.* (2019). [Colour figure can be viewed at wileyonlinelibrary.com]

and Eastern Antarctic Peninsula (Figure 3), explained by the discontinuity of atmospheric moisture transport across the mountains of the Antarctic Peninsula (Slonaker and Van Woert, 1999), which are influenced by the dominant synoptic patterns on the region (Gonzalez *et al.*, 2018). Such exponents around 0.5 can also be found over most of West Antarctica and at the highest regions of the Antarctic Plateau. Instead, the lower exponents are

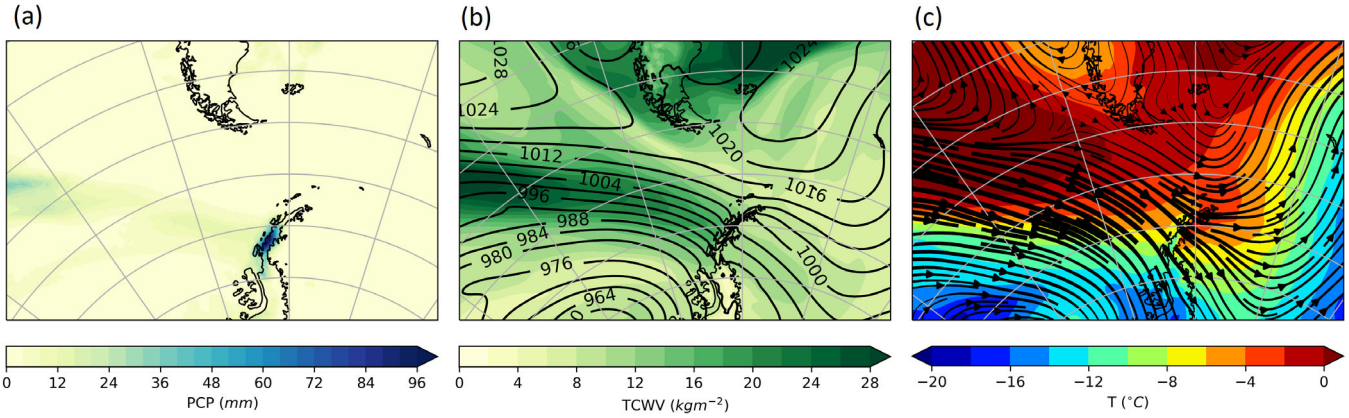

FIGURE 4 Extreme precipitation and average values of selected atmospheric variables on 27 March 2017. (a) Total precipitation, (b) average mean sea level pressure (contours) and total content water vapour (shaded) and, (c) average 700 hPa temperature (shaded) and streamlines. Width of streamlines are proportional to the wind speed. The location of the EPR is shown as a white dot. [Colour figure can be viewed at wileyonlinelibrary.com]

found on the Amery Ice Shelf and west of Victoria Land, where orography blocks moisture transport from the ocean, while strong katabatic flow decrease precipitation via sublimation (Turner *et al*., 2019; Gehring *et al*., 2022).

In general, local scaling coefficients agree well with the contribution of the highest precipitation events to the annual total precipitation (compare Figure 2 in Turner *et al*., 2019, and Figure 2 here). Small scaling exponents are related with the sites where about 50% of the annual precipitation is concentrated in a few days, while large scaling exponents are located where half of the annual precipitation is distributed over a longer period. Extreme precipitation scaling is therefore a good indicator of the contribution of the extreme precipitation events to the annual totals.

5 | EXTREME PRECIPITATION CASE STUDIES

In order to understand the primary processes that shape the EPRs at different temporal scales, this section presents four case studies simulated by ERA5 at 1, 3, 10 days and 1 year. Here we provide the synoptic conditions that provided the most extreme precipitation conditions in the Antarctic Peninsula, where all these records occurred.

5.1 | 27 March 2017 (1-day EPR)

According to ERA5, on 27 March 2017 the grid point with coordinates 66.25°S 64.75°W registered 110 mm, the Antarctic precipitation record in 1 day from 1979 to 2017 (Figure 4a, Figure S3.1.1 and Video S1). The synoptic setting on that day was characterized by the presence of a deep low southeast of the Bellingshausen Sea. This setting triggered the transport of warm moist air from the South-eastern Pacific to the central part of the western Antarctic Peninsula (Figures 4b,c) in a zonally oriented atmospheric river identified over the Southern Ocean the extension of which reached the AP (Video S2). This still intense moisture flux impinged on the steep orography of the region, releasing most of the moisture as precipitation on the western side, while drying at the eastern side of the region by foehn effect. According to SYNOP observations, rainfall was observed at Rothera during that day. ERA5 also simulated rainfall at low levels in all the western coast of the AP (Supplementary Figure S3.1.2).

Although the values of total cloud water content (TCWV) and the dynamic forcing are large (Figure 4b), none of them are extraordinary in the region. High values of vertical velocity and convergence of moisture at the windward of the Antarctic Peninsula (not shown) reveal the predominant role of the orography in this event. The analysis of the cross sections across the mountain shows large values of cloud liquid water content below 2,000 m rising by the effect of the mountain to 6,000 m where the snow water content is enhanced (Figure S3.1.3). We hypothesize that the interaction of snow and ice particles on the windward side of the Antarctic Peninsula mountain range through processes like riming might have increased the precipitation efficiency of the event (see e.g., Gehring *et al*., 2020). In that case precipitation microphysics could have played an important role in achieving extreme amounts of precipitation.

5.2 | 15–17 July 2016 (3-day EPR)

From 15 to 17 July 2016, a grid point on the north Alexander Island (69.00S 70.50W) achieved 221.0 mm of total accumulated precipitation in ERA5 (Figure 5a), recording

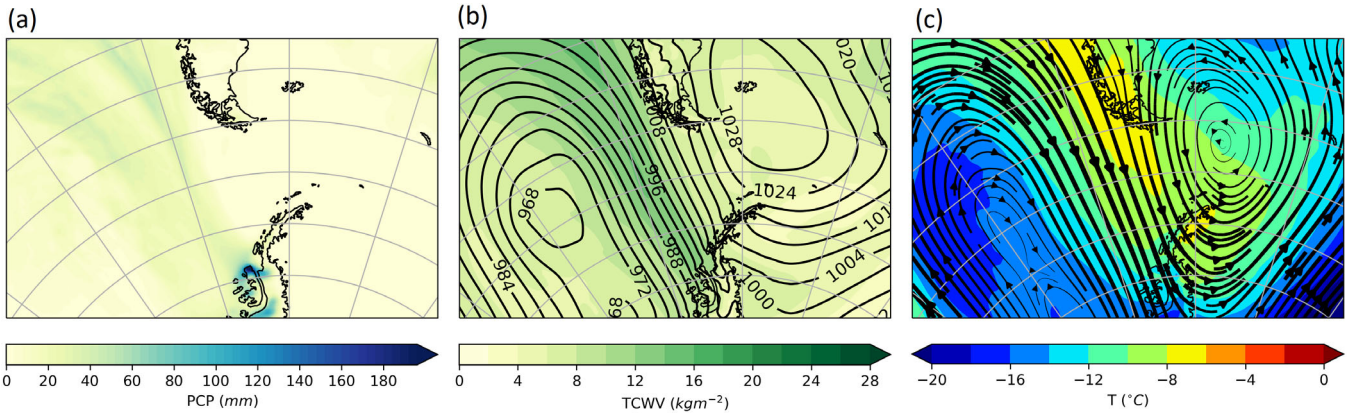

FIGURE 5 As Figure 4 but for the extreme precipitation event averaged on 15–17 July 2016. [Colour figure can be viewed at wileyonlinelibrary.com]

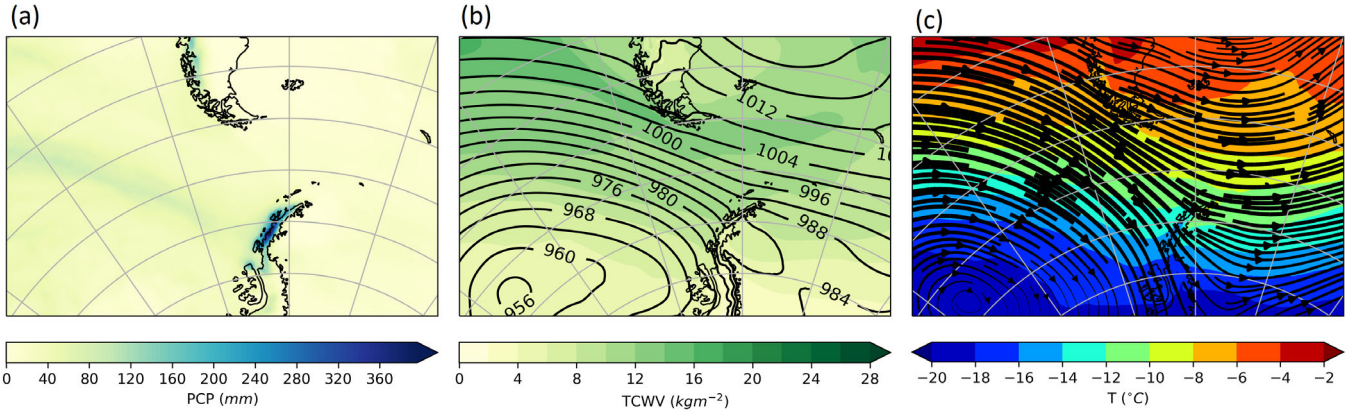

FIGURE 6 As Figure 4 but for the extreme precipitation event averaged on 21–30 September 1996. [Colour figure can be viewed at wileyonlinelibrary.com]

the 3-day most extreme event in this reanalysis from 1979 to 2020. This event is also the most extreme 3-day precipitation event in RACMO2 model, with 488.0 mm in a nearby grid and recording on the 16 July 2016 the most extreme event in 1-day precipitation event in the model. The identification of the same event in both ERA5 reanalysis and RACMO2 reinforces extreme conditions associated with this event.

A key characteristic of this event was the presence of a persistent atmospheric river stretching from north to south pulling warm and moist tropical air from 30°S to 70°S at the Antarctic Peninsula in the winter season (Figure 5b,c and Videos S3 and S4). The atmospheric river lasted all 3 days of the extreme precipitation event with its tail moving from the Pacific Ocean over the southern South America towards the Atlantic, while its front extended towards the Antarctic Peninsula. The atmospheric river was triggered by a stationary deep low over the Bellingshausen Sea, with a blocking ridge in the southwest Atlantic (typical large-scale conditions behind atmospheric river development in the region, Wille *et al.*, 2021). Several secondary lows developed on its northeast flank that moved in a southeast direction impacting the orography of the Antarctic Peninsula (Video S3). The cyclogenesis of these lows, of which one had explosive character (28 hPa decrease in mean sea level pressure in 24 hr) was induced by the potential vorticity at high levels (Figures S3.2.1 and S3.2.2). Secondary lows intensified the initial front present on the 14 July, giving successive warm and cold frontal systems. The dynamic factors were enhanced by the steep orography of the northern side of Alexander Island that, as shown in Figure 5a, was critical for the strong orographic enhancement of the event. Although SYNOP messages and ERA5 reanalysis suggest that snowfall was the predominant precipitation type during this event (Figure S3.2.3) one SYNOP message in Rothera indicated the presence of rainfall during few hours on 17 July.

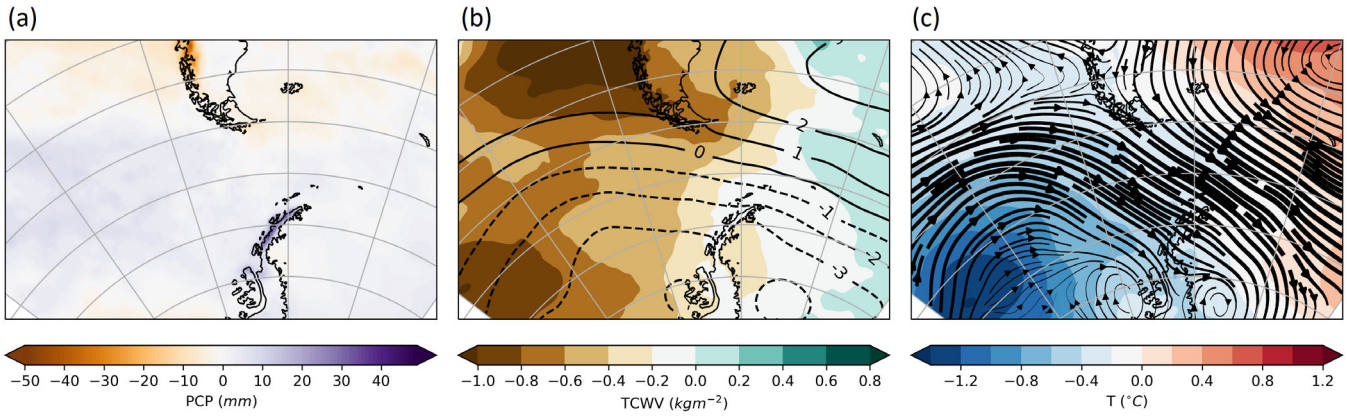

FIGURE 7 Extreme precipitation and average anomalies with respect to the period 1979–2017 of selected atmospheric variables from March 2001 to February 2002. (a) Anomaly of precipitation, (b) anomaly of mean sea level pressure (contours) and total content water vapour (shaded) and, (c) anomaly of 700 hPa temperature (shaded) and streamlines. Width of streamlines are proportional to the wind speed. The location of the EPR is shown as a white dot. [Colour figure can be viewed at wileyonlinelibrary.com]

5.3 | 21–30 September 1996 (10-day EPR)

This EPR event was characterized by a train of cyclones crossing the Bellingshausen Sea producing 425.9 mm over a period of 10 days at the grid point with coordinates 66.00S 64.75W according to ERA5 (Figure 6a). Rainfall was observed at Faraday–Vernadsky station almost continuously during this 10-day period although ERA5 data barely reflect this fact. As in the previous cases, a warm and moist flow from the Pacific prevailed over the Antarctic Peninsula (Figure 6b,c). During the event we can differentiate several primary lows, deep and with great extension between 50° and 70°S, and secondary lows with a short life cycle that were developed at the northeastern flank of the main lows (Figure S3.3.1 and Video S5). Secondary lows exhibited rapid cyclogenesis due to the interaction of the negative potential vorticity anomalies with areas of low-level baroclinicity downstream and presented a meridional track towards the Antarctic Peninsula.

The repeated passage of fronts and the persistent flow of warm and moist air produced large amounts of precipitation enhanced on the windward side of the Antarctic Peninsula by the orography. In this 10-day event, there is not one unique atmospheric river but rather a succession of intense moisture fluxes identified as ARs landfalling at the Peninsula on 23 and 28 September stretching from the Pacific and the Atlantic Ocean, respectively (Video S6). We highlight the cyclogenesis of the 22, 25 and 27th September that developed at low latitudes, and 24 hr later, produced high precipitation amounts over the Antarctic Peninsula.

5.4 | 26 February 2001 to 25 February 2002 (1-year EPR)

According to ERA5, the 1-year precipitation record occurred from February 26, 2001 to February 25, 2002 and took place at the grid point with coordinates 66.00S64.75W (Figure 7a). This period accumulated a total precipitation amount of 4,266.6 mm. We examined this case in terms of anomalies computed using monthly mean values from March 2001 to February 2002 with respect to the period 1979–2017. The 1-year record was characterized by a pressure dipole with negative mean sea level pressure anomaly at the Bellingshausen Sea and positive anomaly over the South Atlantic Ocean. This pattern favoured strong south-eastward flow from southeast Pacific to Antarctic Peninsula (Figure 7b,c). Negative temperature anomalies at the Bellingshausen Sea (Figure 7c) were associated with low values of TCWV (Figure 7b). Despite the relatively dry advection at climate timescales on the Antarctic Peninsula, positive precipitation anomalies are observed being enhanced by the mountains at the northern sector (Figure 7a). This suggest that the primary contribution for large-scale precipitation extremes during this year was the strong circulation impinging the Antarctic Peninsula Mountains. Alternatively, several intense moisture advection events with an overall dry mean for the year might also explain this pattern.

6 | CONCLUSIONS

Records of extreme precipitation occur when all atmospheric ingredients that produce precipitation are

optimized. In Antarctica, extreme precipitation records concentrate in the middle sector of the Antarctic Peninsula as revealed by ERA5 and RACMO2 datasets. The combination of latitude, orography and the presence of atmospheric rivers impinging the mountains may produce precipitation events with more than 100 mm in 1 day according to both datasets. The lack of summer events evidences that local moisture sources do not play a key role on extreme precipitation. At scales of months and years, a south-eastward circulation anomaly increasing the air advection from southeast Pacific perpendicular to Antarctic Peninsula causes precipitation events comparable to mid-latitude regions. These structures are regular in time and despite the internal variability of the precipitation, different wet spells from synoptic systems crossing the Antarctic Peninsula contribute to the extreme precipitation records at large temporal scales in the region.

Scaling law exponents of EPR indicate the regularity of extreme precipitation events in the continent, being higher in the Southern Ocean ($b \sim 0.7$) and lower in some areas of the East Antarctic Ice Sheet ($b \sim 0.3$). Exponent is especially low at the Amery Ice Shelf and west of Victoria Land coinciding with the lower contribution of the extreme precipitation events to the annual totals (Turner *et al.*, 2019). The Antarctic Peninsula exhibits a pronounced discontinuity with higher values in the Bellingshausen Sea and lower values in the Weddell Sea.

We acknowledge that the use of reanalysis and model data may be the main limitation of this research. However, currently there is no alternative to study the precipitation around Antarctica at the daily scale due to the scarce and biased surface observations and irregular satellite crossings. The precipitation described by different reanalyses and models shows important differences in magnitude (Bromwich *et al.*, 2011; Tang *et al.*, 2018b). This is evidenced by the differences shown by RACMO2 and ERA5 in the maximum precipitation amounts reported here, which are about a factor 2 higher in RACMO2 than in ERA5. Nonetheless, we found that some of the extreme events simulated by RACMO2 coincide with ERA5, and that the spatial distribution of the power law scaling exponent is coherent between both reanalyses. This strongly suggests that, regardless of differences in the precipitation amounts, global patterns of EPRs are well captured and individual extreme events can be identified with a reasonable degree of confidence.

In this investigation, we show the approximate values of the precipitation at different temporal scales in Antarctica, and we present the synoptic atmospheric mechanisms that produce such extreme events. Extreme precipitation events, such as those presented in this study, determine an important part of the variability of the snow accumulation on the Antarctic ice sheet and have the potential for impacting the Antarctic ecological systems (e.g., displacing a penguin colony). Our results intend to be a benchmark to characterize extreme precipitation events in Antarctica and monitor its change, as well as their impacts in the Antarctic ecosystem.

AUTHOR CONTRIBUTIONS

Sergi González-Herrero: Conceptualization; methodology; investigation; writing – review and editing; writing – original draft; visualization; software. **Francisco Vasallo:** Investigation; visualization; writing – review and editing. **Joan Bech:** Methodology; investigation; writing – review and editing. **Irina Gorodetskaya:** Investigation; writing – review and editing. **Benito Elvira:** Investigation; writing – review and editing. **Ana Justel:** Investigation; writing – review and editing.

ACKNOWLEDGEMENTS

This is a contribution to the Year of Polar Prediction (YOPP), a flagship activity of the Polar Prediction Project (PPP), initiated by the World Weather Research Programme (WWRP) of the World Meteorological Organization (WMO) and to the Scientific Committee on Antarctic Research (SCAR) scientific research programme "Near-term Variability and Prediction of the Antarctic Climate System" (AntClimNow). AEMET Antarctic programme is supported by the MSIU (Spain). This work was funded by the Spanish Agencia Estatal de Investigación (AEI) and Fondo Europeo al Desarrollo Regional (FEDER) (grant numbers CGL2015-65627-C3-1-R, CGL2015-65627-C3-2-R, RTI2018-098693-B-C32, PID2020-116520RB-I00). Research activities of Sergi González-Herrero are partly supported by ANTALP Research Group (2021 SGR 00269), Generalitat de Catalunya. Irina Gorodetskaya thanks the support by the strategic funding to CESAM (grant numbers UIDP/50017/2020, UIDB/50017/2020 and LA/P/0094/2020), CIIMAR (UIDB/04423/2020, UIDP/04423/2020), 2021.03140.CEECIND and Project ATLACE (CIRCNA/-CAC/0273/2019) through national funds provided by FCT—Fundação para a Ciência e a Tecnologia. Open access funding provided by ETH-Bereich Forschungsanstalten.

DATA AVAILABILITY STATEMENT

Data used in this study are publicly accessible. ERA5 dataset can be downloaded from: https://cds.climate.copernicus.eu/. RACMO2 dataset can be downloaded from: https://doi.org/10/c2pv. The code for the AR detection algorithm used in supplementary videos is available via Jonathan Wille (2020), jwille45/Antarctic-lab: v2.3

(v2.3), Zenodo, https://doi.org/10.5281/zenodo.4009663. The dataset generated in this research with the precipitation extremes for each model at every grid point and for different durations are available via Gonzalez-Herrero (2022), Extreme precipitation records in Antarctica [Dataset], Zenodo, https://doi.org/10.5281/zenodo.7538266. The codes used in this study are available via Gonzalez-Herrero (2022), Extreme precipitation records in Antarctica [Code] Zenodo, https://doi.org/10.5281/zenodo.7573644.

REFERENCES

Behrangi, A., Christensen, M., Richardson, M., Lebsock, M., Stephens, G., Huffman, G.J. et al. (2016) Status of high-latitude precipitation estimates from observations and reanalyses. *Journal of Geophysical Research: Atmospheres*, 121(9), 4468–4486. Available from: https://doi.org/10.1002/2015JD024546

Boisvert, L.N., Webster, M.A., Petty, A.A., Markus, T., Cullather, R. I. & Bromwich, D.H. (2020) Intercomparison of precipitation estimates over the southern ocean from atmospheric reanalyses. *Journal of Climate*, 33(24), 10627–10651. Available from: https://doi.org/10.1175/JCLI-D-20-0044.1

BOM. (2022) Rainfall and temperature records. Bureau of Meteorology. Available at: https://www.bom.gov.au/climate/extreme/records.shtml [Accessed December 24, 2022]

Breña-Naranjo, J.A., Pedrozo-Acuña, A. & Rico-Ramirez, M.A. (2015) World's greatest rainfall intensities observed by satellites. In: *Atmospheric Science Letters*. Wiley-Blackwell, 16, 420–424. https://doi.org/10.1002/asl2.546

Bromwich, D.H., Guo, Z., Bai, L. & Chen, Q.S. (2004) Modeled Antarctic precipitation. Part I: spatial and temporal variability. *Journal of Climate*, 17(3), 427–447. Available from: https://doi.org/10.1175/1520-0442(2004)017<0427:MAPPIS>2.0.CO;2

Bromwich, D.H., Nicolas, J.P. & Monaghan, A.J. (2011) An assessment of precipitation changes over Antarctica and the southern ocean since 1989 in contemporary global reanalyses. *Journal of Climate*, 24(16), 4189–4209. Available from: https://doi.org/10.1175/2011JCLI4074.1

Casas, M.C., Rodríguez, R. & Redaño, Á. (2010) Analysis of extreme rainfall in Barcelona using a microscale rain gauge network. *Meteorological Applications*, 17(1), 117–123. Available from: https://doi.org/10.1002/met.166

Cerveny, R.S., Lawrimore, J., Edwards, R. & Landsea, C. (2007) Extreme weather records: compilation, adjudication, and publication. *Bulletin of the American Meteorological Society*, 88(6), 853–860. Available from: https://doi.org/10.1175/BAMS-88-6-853

Corral, Á., Ossó, A. & Llebot, J.E. (2010) Scaling of tropical-cyclone dissipation. *Nature Physics*, 6(9), 693–696. Available from: https://doi.org/10.1038/nphys1725

Dalaiden, Q., Goosse, H., Lenaerts, J.T.M., Cavitte, M.G.P. & Henderson, N. (2020) Future Antarctic snow accumulation trend is dominated by atmospheric synoptic-scale events. *Communications Earth & EnvironmentNature Publishing Group*, 1(1), 1–9. Available from: https://doi.org/10.1038/s43247-020-00062-x

Espinoza, V., Waliser, D.E., Guan, B., Lavers, D.A. & Ralph, F.M. (2018) Global analysis of climate change projection effects on atmospheric rivers. *Geophysical Research Letters*, 45(9), 4299–4308. Available from: https://doi.org/10.1029/2017GL076968

Folland, C.K. (1988) Numerical models of the raingauge exposure problem, field experiments and an improved collector design. *Quarterly Journal of the Royal Meteorological Society*, 114, 1485–1516. Available from: https://doi.org/10.1002/qj.49711448407

Frieler, K., Clark, P.U., He, F., Buizert, C., Reese, R., Ligtenberg, S. R.M. et al. (2015) Consistent evidence of increasing Antarctic accumulation with warming. *Nature Climate Change*, 5, 348–352. Available from: https://doi.org/10.1038/nclimate2574

Galmarini, S., Steyn, D.G. & Ainslie, B. (2004) The scaling law relating world point-precipitation records to duration. *International Journal of Climatology*, 24(5), 533–546. Available from: https://doi.org/10.1002/joc.1022

Gehring, J., Oertel, A., Vignon, É., Jullien, N., Besic, N. & Berne, A. (2020) Microphysics and dynamics of snowfall associated with a warm conveyor belt over Korea. *Atmospheric Chemistry and Physics*, 20(12), 7373–7392. Available from: https://doi.org/10.5194/ACP-20-7373-2020

Gehring, J., Vignon, É., Billault-Roux, A.C., Ferrone, A., Protat, A., Alexander, S.P. et al. (2022) Orographic flow influence on precipitation during an atmospheric river event at Davis, Antarctica. *Journal of Geophysical Research: Atmospheres*, 127(2), e2021JD035210. Available from: https://doi.org/10.1029/2021JD035210

Gonzalez, S. & Bech, J. (2017) Extreme point rainfall temporal scaling: a long term (1805–2014) regional and seasonal analysis in Spain. *International Journal of Climatology*, 37(15), 5068–5079. Available from: https://doi.org/10.1002/joc.5144

Gonzalez, S., Vasallo, F., Recio-Blitz, C., Guijarro, J.A. & Riesco, J. (2018) Atmospheric patterns over the Antarctic Peninsula. *Journal of Climate*, 31(9), 3597–3608. Available from: https://doi.org/10.1175/JCLI-D-17-0598.1

Gorodetskaya, I.V., Tsukernik, M., Claes, K., Ralph, M.F., Neff, W. D. & Van Lipzig, N.P.M. (2014) The role of atmospheric rivers in anomalous snow accumulation in East Antarctica. *Geophysical Research Letters*, 41(17), 6199–6206. Available from: https://doi.org/10.1002/2014GL060881

Gorodetskaya, I.V., Kneifel, S., Maahn, M., Thiery, W., Schween, J. H., Mangold, A. et al. (2015) Cloud and precipitation properties from ground-based remote-sensing instruments in East Antarctica. *The Cryosphere*, 9(1), 285–304. Available from: https://doi.org/10.5194/tc-9-285-2015

Hersbach, H., Bell, B., Berrisford, P., Hirahara, S., Horányi, A., Muñoz-Sabater, J. et al. (2020) The ERA5 global reanalysis. *Quarterly Journal of the Royal Meteorological Society*, 146, 1999–2049. Available from: https://doi.org/10.1002/qj.3803

Hubert, P., Tessier, Y., Lovejoy, S., Schertzer, D., Schmitt, F., Ladoy, P. et al. (1993) Multifractals and extreme rainfall events. *Geophysical Research Letters*, 20(10), 931–934. Available from: https://doi.org/10.1029/93GL01245

Jennings, A.H. (1950) World's greatest observed point rainfalls. *Monthly Weather Review*, 78(1), 4–5. Available from: https://doi.org/10.1175/1520-0493(1950)078<0004:WGOPR>2.0.CO;2

Kochendorfer, J., Rasmussen, R., Wolff, M., Baker, B., Hall, M.E., Meyers, T. et al. (2017) The quantification and correction of wind-induced precipitation measurement errors. *Hydrology and Earth System Sciences*, 21, 1973–1989. Available from: https://doi.org/10.5194/hess-21-1973-2017

Koutsoyiannis, D. & Papalexiou, S.M. (2017) Extreme rainfall: global perspective. In: *Handbook of Applied Hydrology*. New York, NY: McGraw-Hill, pp. 74–71.

Krinner, G., Magand, O., Simmonds, I., Genthon, C. & Dufresne, J. L. (2007) Simulated Antarctic precipitation and surface mass balance at the end of the twentieth and twenty-first centuries. *Climate Dynamics*, 28(2–3), 215–230. Available from: https://doi.org/10.1007/s00382-006-0177-x

Lenaerts, J.T.M., Van Den Broeke, M.R., Van De Berg, W.J., Van Meijgaard, E. & Kuipers, M.P. (2012) A new, high-resolution surface mass balance map of Antarctica (1979–2010) based on regional atmospheric climate modeling. *Geophysical Research Letters*, 39(4), L04501. Available from: https://doi.org/10.1029/2011GL050713

Lenaerts, J.T.M., Vizcaino, M., Fyke, J., van Kampenhout, L. & van den Broeke, M.R. (2016) Present-day and future Antarctic ice sheet climate and surface mass balance in the community earth system model. *Climate Dynamics*, 47(5–6), 1367–1381. Available from: https://doi.org/10.1007/S00382-015-2907-4/FIGURES/13

Ligtenberg, S.R.M., van de Berg, W.J., van den Broeke, M.R., Rae, J. G.L. & van Meijgaard, E. (2013) Future surface mass balance of the Antarctic ice sheet and its influence on sea level change, simulated by a regional atmospheric climate model. *Climate Dynamics*, 41(3–4), 867–884. Available from: https://doi.org/10.1007/S00382-013-1749-1

McPhillips, L.E., Chang, H., Chester, M.V., Depietri, Y., Friedman, E., Grimm, N.B. et al. (2018) Defining extreme events: a cross-disciplinary review. *Earth's Future*, 6(3), 441–455. Available from: https://doi.org/10.1002/2017EF000686

Mottram, R., Hansen, N., Kittel, C., Van Wessem, J.M., Agosta, C., Amory, C. et al. (2021) What is the surface mass balance of Antarctica? An intercomparison of regional climate model estimates. *Cryosphere*, 15(8), 3751–3784. Available from: https://doi.org/10.5194/tc-15-3751-2021

Nicolas, J.P., Vogelmann, A.M., Scott, R.C., Wilson A.B., Cadeddu, M.P., Bromwich, D.H., Verlinde, J., Lubin, D., Russell, L.M., Jenkinson, C., Powers, H.H., Ryczek, M., Stone, G., Wille, J.D. et al. (2017) January 2016 extensive summer melt in West Antarctica favoured by strong El Niño. *Nature Communications*, 8, 15799. Available from: https://doi.org/10.1038/ncomms15799

NWS. (2022a) HDSC world record point precipitation measurements. National Weather Service. National Oceanic and Atmospheric Administration (NOAA). Available at: https://www.weather.gov/owp/hdsc_world_record [Accessed December 24, 2022]

NWS. (2022b) HDSC USA record point precipitation measurements. National Weather Service. National Oceanic and Atmospheric Administration (NOAA). Available at: https://www.weather.gov/owp/hdsc_usa_record [Accessed December 24, 2022]

O'brien, T.A., Wehner, M.F., Payne, A.E., Shields, C.A., Rutz, J.J., Leung, L.-R. et al. (2022) Increases in future AR count and size: overview of the ARTMIP tier 2 CMIP5/6 experiment. *Journal of Geophysical Research: Atmospheres*, 127(6), e2021JD036013. Available from: https://doi.org/10.1029/2021JD036013

Parish, T.R. & Bromwich, D.H. (2007) Reexamination of the near-surface airflow over the Antarctic continent and implications on atmospheric circulations at high southern latitudes. *Monthly Weather Review*, 135(5), 1961–1973. Available from: https://doi.org/10.1175/MWR3374.1

Paulhus, J.L.H. (1965) Indian Ocean and Taiwan rainfalls set new records. *Monthly Weather Review*, 93(5), 331–335. Available from: https://doi.org/10.1175/1520-0493(1965)093<0331:IOATRS>2.3.CO;2

Pérez-Zanón, N., Casas-Castillo, M.C., Rodríguez-Solà, R., Peña, J. C., Rius, A., Solé, J.G. et al. (2016) Analysis of extreme rainfall in the Ebre Observatory (Spain). *Theoretical and Applied Climatology*, 124(3–4), 935–944. Available from: https://doi.org/10.1007/s00704-015-1476-0

Peters, O. & Christensen, K. (2002) Rain: relaxations in the sky. *Physical Review E—Statistical Physics, Plasmas, Fluids, and Related Interdisciplinary Topics*, 66(3), 036120. Available from: https://doi.org/10.1103/PhysRevE.66.036120

Peters, O., Hertlein, C., Christensen, K. & Hertlein, C. (2002) A complexity view of rainfall. *Physical Review Letters*, 88(1), 4. Available from: https://doi.org/10.1103/PhysRevLett.88.018701

Pöschmann, J.M., Kim, D., Kronenberg, R. & Bernhofer, C. (2021) An analysis of temporal scaling behaviour of extreme rainfall in Germany based on radar precipitation QPE data. *Natural Hazards and Earth System Sciences*, 21(4), 1195–1207. Available from: https://doi.org/10.5194/nhess-21-1195-2021

Quetelard, H., Bessemoulin, P., Cerveny, R.S., Peterson, T.C., Burton, A. & Boodhoo, Y. (2009) Extreme weather: world-record rainfalls during tropical cyclone gamede. *Bulletin of the American Meteorological Society*, 90(5), 603–608. Available from: https://doi.org/10.1175/2008BAMS2660.1

Rawlings, J.O., Pantula, S.G. & Dickey, D.A. (1998) *Applied Regression Analysis*. New York, NY: Springer-Verlag.

Roussel, M.L., Lemonnier, F., Genthon, C. & Krinner, G. (2020) Brief communication: evaluating Antarctic precipitation in ERA5 and CMIP6 against CloudSat observations. *The Cryosphere*, 14(8), 2715–2727. Available from: https://doi.org/10.5194/tc-14-2715-2020

Schlosser, E., Powers, J.G., Duda, M.G., Manning, K.W., Reijmer, C. H. & van den Broeke, M.R. (2010) An extreme precipitation event in Dronning Maud Land, Antarctica: a case study with the Antarctic mesoscale prediction system. *Polar Research*, 29(3), 330–344. Available from: https://doi.org/10.3402/polar.v29i3.6072

Slonaker, R.L. & Van Woert, M.L. (1999) Atmospheric moisture transport across the Southern Ocean via satellite observations. *Journal of Geophysical Research Atmospheres*, 104(D8), 9229–9249. Available from: https://doi.org/10.1029/1999JD900045

Tang, M.S.Y., Chenoli, S.N., Colwell, S., Grant, R., Simms, M., Law, J. et al. (2018a) Precipitation instruments at Rothera Station, Antarctic Peninsula: a comparative study. *Polar Research*, 37(1), 1503906. Available from: https://doi.org/10.1080/17518369.2018.1503906

Tang, M.S.Y., Chenoli, S.N., Samah, A.A. & Hai, O.S. (2018b) An assessment of historical Antarctic precipitation and temperature trend using CMIP5 models and reanalysis datasets. *Polar Science*, 15, 1–12. Available from: https://doi.org/10.1016/j.polar.2018.01.001

Tiedtke, M. (1993) Representation of clouds in large-scale models. *Monthly Weather Review*, 121(11), 3040–3061. Available from: https://doi.org/10.1175/1520-0493(1993)121<3040:ROCILS>2.0.CO;2

Turner, J., Lachlan-Cope, T.A., Thomas, J.P. & Colwell, S.R. (1995) The synoptic origins of precipitation over the Antarctic Peninsula. *Antarctic Science*, 7(3), 327–337. Available from: https://doi.org/10.1017/S0954102095000447

Turner, J., Phillips, T., Thamban, M., Rahaman, W., Marshall, G.J., Wille, J.D. et al. (2019) The dominant role of extreme precipitation events in Antarctic snowfall variability. *Geophysical Research Letters*, 46(6), 3502–3511. Available from: https://doi.org/10.1029/2018GL081517

Uotila, P., Lynch, A.H., Cassano, J.J. & Cullather, R.I. (2007) Changes in Antarctic net precipitation in the 21st century based on Intergovernmental Panel on Climate Change (IPCC) model scenarios. *Journal of Geophysical Research Atmospheres*, 112(10), 10107. Available from: https://doi.org/10.1029/2006JD007482

Vignon, R.M.L., Gorodetskaya, I.V., Genthon, C. & Berne, A. (2021) Present and future of rainfall in Antarctica. *Geophysical Research Letters*, 48(8), e2020GL092281. Available from: https://doi.org/10.1029/2020GL092281

Wang, Y., Ding, M., van Wessem, J.M., Schlosser, E., Altnau, S., van den Broeke, M.R. et al. (2016) A comparison of Antarctic ice sheet surface mass balance from atmospheric climate models and in situ observations. *Journal of Climate*, 29(14), 5317–5337. Available from: https://doi.org/10.1175/JCLI-D-15-0642.1

van Wessem, J.M., Reijmer, C.H., Morlighem, M., Mouginot, J., Rignot, E., Medley, B. et al. (2014) Improved representation of East Antarctic surface mass balance in a regional atmospheric climate model. *Journal of Glaciology*, 60(222), 761–770. Available from: https://doi.org/10.3189/2014JOG14J051

Wille, J.D., Favier, V., Gorodetskaya, I.V., Agosta, C., Kittel, C., Beeman, J.C. et al. (2021) Antarctic atmospheric river climatology and precipitation impacts. *Journal of Geophysical Research: Atmospheres*, 126(8), e2020JD033788. Available from: https://doi.org/10.1029/2020JD033788

WMO. (2022) *World Meteorological Organization Global Weather & Climate Extremes Archive*. Available at: https://wmo.asu.edu/content/world-meteorological-organization-global-weather-climate-extremes-archive

Yu, L., Yang, Q., Vihma, T., Jagovkina, S., Liu, J., Sun, Q. et al. (2018) Features of extreme precipitation at Progress Station, Antarctica. *Journal of Climate*, 31(22), 9087–9105. Available from: https://doi.org/10.1175/JCLI-D-18-0128.1

Zhang, H., Fraedrich, K., Blender, R. & Zhu, X. (2013a) Precipitation extremes in CMIP5 simulations on different time scales. *Journal of Hydrometeorology*, 14(3), 923–928. Available from: https://doi.org/10.1175/JHM-D-12-0181.1

Zhang, H., Fraedrich, K., Zhu, X., Blender, R. & Zhang, L. (2013b) World's greatest observed point rainfalls: Jennings (1950) scaling law. *Journal of Hydrometeorology*, 14(6), 1952–1957. Available from: https://doi.org/10.1175/JHM-D-13-074.1

SUPPORTING INFORMATION

Additional supporting information can be found online in the Supporting Information section at the end of this article.

How to cite this article: González-Herrero, S., Vasallo, F., Bech, J., Gorodetskaya, I., Elvira, B., & Justel, A. (2023). Extreme precipitation records in Antarctica. *International Journal of Climatology*, 1–14. https://doi.org/10.1002/joc.8020